

FUSE LIMITS ON FUV EMISSION FROM WARM GAS IN CLUSTERS OF GALAXIES¹

W. VAN DYKE DIXON², SHAUNA SALLMEN, AND MARK HURWITZ
Space Sciences Laboratory
University of California, Berkeley, CA 94720-7450, USA
vand, sallmen, markh@ssl.berkeley.edu

AND

RICHARD LIEU
Department of Physics
University of Alabama in Huntsville, Huntsville, AL 35899, USA
lieur@cspars.uah.edu

To appear in The Astrophysical Journal, Letters

ABSTRACT

We have obtained FUV spectra of two clusters of galaxies with *FUSE*, the *Far Ultraviolet Spectroscopic Explorer*. The Coma cluster was observed for a total of 28.6 ksec, the Virgo cluster for 10.9 ksec. Neither spectrum shows significant O VI $\lambda\lambda 1032, 1038$ emission at the cluster redshift. Such emission would be expected from the warm $[(5 - 10) \times 10^5 \text{ K}]$ component of the intracluster medium (ICM) that has been proposed to explain the excess EUV and SXR flux present in *EUVE* and *ROSAT* observations of these clusters. Our $2\text{-}\sigma$ upper limits on the O VI $\lambda 1032$ flux from Coma and Virgo exclude all published warm-gas models of the EUV excess in these clusters.

Subject headings: galaxies: clusters: general — ultraviolet: galaxies

1. INTRODUCTION

Recent observations with the *Extreme Ultraviolet Explorer* (*EUVE*) provide evidence that a number of clusters of galaxies are strong emitters of EUV radiation (Lieu et al. 1996a,b; Bowyer et al. 1997; Mittaz et al. 1998). This emission is substantially brighter than would be expected from the well-known, X-ray-emitting intracluster medium (ICM; Forman & Jones 1982). Signatures of this “soft excess” are sometimes present in the lowest energy-resolution band of the *ROSAT* PSPC, but its presence remains controversial (Arabadjis & Bregman 1999; Drake 1999; Krick et al. 2000). At present, two groups agree that an EUV excess exists in both the Virgo and Coma clusters, but they differ on the intensity and morphology of the emitting regions (Lieu et al. 1999; Enßlin et al. 1999; Bowyer & Berghöfer 1998; Bowyer et al. 1999; Berghöfer et al. 2000).

The EUV excess in clusters of galaxies was originally attributed to a diffuse, $(5 - 10) \times 10^5 \text{ K}$ thermal gas component of the ICM. Gas at these temperatures cools rapidly, however, requiring either a substantial mass of cooling gas or a heretofore unknown energy source to reheat it (Fabian 1996). If a reservoir of warm gas were present in the cores of clusters of galaxies, it would emit strongly in the far-UV (FUV) resonance lines of O VI $\lambda\lambda 1032, 1038$ and C IV $\lambda\lambda 1548, 1551$ as it cools through temperatures of a few times 10^5 K (Edgar & Chevalier 1986; Voit et al. 1994), yet Dixon et al. (1996) were unable to detect either doublet in the spectra of five clusters of galaxies obtained with the Hopkins Ultraviolet Telescope (HUT). To probe more deeply for this emission, we have observed the Virgo and Coma clusters with the *Far Ultraviolet Spectroscopic Explorer* (*FUSE*). Our limits on the O VI flux of each cluster

place tight constraints on the emission integral of any warm component of their ICM.

2. OBSERVATIONS AND DATA REDUCTION

FUSE comprises four separate optical systems. Two employ LiF optical coatings and are sensitive to wavelengths from 990 to 1187 Å, while the other two use SiC coatings, which provide reflectivity to wavelengths as short as 905 Å. The four channels overlap between 990 and 1070 Å. For a complete description of *FUSE*, see Moos et al. (2000) and Sahnou et al. (2000).

The *FUSE* spectrum of the Coma cluster was obtained in 17 separate exposures on 2000 June 18 and 19. Each was centered on $12^{\text{h}}59^{\text{m}}49^{\text{s}}.0, +27^{\circ}57'46''$ (J2000, or $l = 57.61, b = +87.96$ in Galactic coordinates), near the cluster center. The total exposure was 28608 s, with 23553 s obtained during orbital night. We use the entire 29-ksec data set in our analysis. Our spectrum of the Virgo cluster is a combination of data from two locations near the cluster center. Two exposures, centered on $12^{\text{h}}31^{\text{m}}07^{\text{s}}.3, +12^{\circ}23'46''$ ($l = 284.03, b = +74.52$) and totaling 2242 s, were obtained on 2000 June 13. Seven exposures, centered on $12^{\text{h}}31^{\text{m}}13^{\text{s}}.4, +12^{\circ}22'10''$ ($l = 284.2, b = +74.50$) and totaling 8688 s, were obtained on 2000 June 17. The total integration time is 10,930 s, all of it during orbital night. All observations were made through the $30'' \times 30''$ (LWRS) aperture.

The standard *FUSE* data-reduction software are used to confirm that none of our data were obtained during passages through the South Atlantic Anomaly or at low earth-limb angles, to separate day and night observations, and to confirm that the dead-time correction for both observations is negligible. To reduce the detector background,

¹ Based on observations made with the NASA-CNES-CSA *Far Ultraviolet Spectroscopic Explorer*. *FUSE* is operated for NASA by the Johns Hopkins University under NASA contract NAS5-32985.

² Current address: Department of Physics and Astronomy, The Johns Hopkins University, Baltimore, MD 21218, USA

photon events with pulse heights less than 4 or greater than 15 (in standard arbitrary units) are excluded from the data set. Subsequent data reduction is performed by hand. Photon events from regions of the detector with known defects are removed. The standard extraction window defined for the LWRS aperture is centered (in the dimension perpendicular to the dispersion axis) on the diffuse airglow emission lines.

While the resolution of the *FUSE* spectrograph is approximately 15 km s^{-1} for a point source, diffuse emission filling the LWRS aperture yields a line profile that is well approximated by a top-hat function with a width of $\sim 106 \text{ km s}^{-1}$. Our spectra are quite faint, so we bin the Coma data by 8 detector pixels, or about 15.5 km s^{-1} . We bin the data from the shorter Virgo observation by 16 pixels. We distinguish between detector pixels and 8- or 16-pixel bins throughout this paper.

We omit the final steps of the standard *FUSE* data-reduction pipeline for several reasons: first, the pipeline’s corrections for differential Doppler shifts and grating and electronics drifts total less than 10 detector pixels in the dispersion direction. Second, the distortion correction, applied independently for each of the instrument apertures, can cause background photons to “pile up” in the region between two nominal extraction windows, forming a horizontal stripe in the processed detector image. These stripes occasionally overlap our preferred extraction window. For bright point sources, this effect is unimportant, but for faint, diffuse sources, we prefer not to risk including such features in our extracted spectrum. Finally, we wish to include the detector background as a free parameter in our spectral models, so forgo the background subtraction steps included in the standard pipeline.

The *FUSE* flux calibration, based on theoretical models of white-dwarf stellar atmospheres, is believed accurate to about 10% (Sahnou et al. 2000). Corrections to the nominal *FUSE* wavelength scale are derived from the measured positions of airglow features in each detector segment and are good to about 0.01 \AA . In practice, only the portion of the Coma spectrum obtained during orbital day contains airglow features strong enough to allow an independent wavelength correction. We thus apply the Coma correction to the Virgo data; the resulting wavelength solution is consistent (within the errors) with the positions of measurable airglow lines. Error bars are assigned to the data assuming Gaussian statistics, then smoothed by 9 bins to remove small-scale features in the error spectrum without significantly changing its shape. Segments of the flux- and wavelength-calibrated LiF 1A spectra, showing O VI $\lambda\lambda 1032, 1038$ at the redshift of each cluster, are presented in Fig. 1. We assume $z = 0.0231$ for Coma (Struble & Rood 1999) and $z = 0.0036$ for Virgo (Ebeling et al. 1998). Diffuse emission from our own Galaxy is present in both spectra; these results are presented in Dixon et al. (2001).

3. SPECTRAL ANALYSIS

In our analysis, model spectra are fit to the flux-calibrated data using the nonlinear curve-fitting program SPECFIT (Kriss 1994), which runs in the IRAF³ environment, to perform a χ^2 minimization of the model param-

eters. We find that, because of the wide disparity in the effective area of the various detector segments, combining spectra from different segments does not significantly improve the signal-to-noise ratio. We thus use data only from the segment with the highest effective area at the wavelength of interest.

To set limits on the flux of an emission feature, we first fit a linear continuum to the spectrum. We then add a synthetic emission feature to the data array, raising its flux until χ^2 for the best-fit model with an emission feature differs from χ^2 for the best-fit model without an emission feature by $\Delta\chi^2 = 9$ (corresponding to a $3\text{-}\sigma$ deviation for one interesting parameter, in this case the flux in the emission line; Avni 1976). We quote as a $3\text{-}\sigma$ upper limit the flux of the model emission line that best fits the synthetic emission feature originally added to the data. Upper limits derived in this way are unaffected by small-scale features in the observed continua. The best-fit linear continuum and our $3\text{-}\sigma$ upper limits to the flux of the O VI doublet for each cluster are shown in Fig. 1.

The observed profile of a diffuse emission feature represents a convolution of its intrinsic profile with the 106 km s^{-1} top-hat function discussed above. In our models, we assume the intrinsic profile to be a Gaussian with FWHM = 40 km s^{-1} , corresponding to the thermal width of a $5 \times 10^5 \text{ K}$ gas. Broader lines, perhaps due to bulk motions in the gas, would yield higher upper limits, as the flux is spread over a greater region of the detector. For example, lines with an intrinsic FWHM = 200 km s^{-1} yield upper limits approximately 70% higher than those of 40 km s^{-1} lines.

No significant FUV line emission is seen at the cluster redshift in either spectrum. Our limits on the fluxes of various lines predicted to be strong in thermal-gas (Landini & Monsignori Fossi 1990), mixing-layer (Slavin et al. 1993), and shock (Hartigan et al. 1987) models are presented in Table 1. Dereddened intensities are calculated assuming the extinction parameterization of Cardelli et al. (1989, hereafter CCM) with $E(B-V) = 0.008$ for Coma and 0.030 for Virgo (Schlegel et al. 1998) and $R_V = 3.1$. Uncertainties in the reddening correction are discussed in Dixon et al. (1996).

At the wavelength of redshifted O VI in the Coma cluster ($1055.77, 1061.59 \text{ \AA}$), the LiF 1A detector channel has an effective area $A_{\text{eff}} = 24.3 \text{ cm}^{-2}$, by far the highest of the four *FUSE* channels (Sahnou et al. 2000). Unfortunately, a bright band of scattered light contaminates the LiF 1A spectrum from about 1045 to 1058 \AA . Present even at night, the band is clearly visible in Fig. 1. It shows considerable structure, including an apparent emission feature at 1054.5 \AA . Because the intensity of the band varies on small spatial scales, background spectra extracted from detector regions above and below our spectral window cannot be used to predict its shape in our spectrum. The statistical significance of the 1054.5 \AA feature is about 3.3σ ; if real, it should be present in the spectrum from the less-sensitive ($A_{\text{eff}} = 15.5 \text{ cm}^{-2}$) LiF 2B channel at a significance of $> 2 \sigma$. No such feature is seen, and we conclude that it is an artifact of the stray-light stripe in the LiF 1A detector segment.

³ The Image Reduction and Analysis Facility (IRAF) is distributed by the National Optical Astronomy Observatories, which is operated by the Association of Universities for Research in Astronomy, Inc., (AURA) under cooperative agreement with the National Science Foundation.

Because the *FUSE* SiC channels lie on the sun-illuminated side of the spacecraft, their spectra may be contaminated by solar emission (Shelton et al. 2001). We thus use only data obtained during orbital night to set limits on emission features in these spectra. In practice, only the S VI $\lambda 933.38$ line in our Coma spectrum is affected, as all other features in the spectrum are redshifted onto the LiF detector channels. All of the Virgo data were obtained during orbital night.

In our Virgo spectrum, the C II* $\lambda 1037.02$ and O VI $\lambda 1037.62$ lines are redshifted to 1040.75 and 1041.36 Å, respectively, and, if present, might be contaminated by flux from the O I airglow features at 1040.94 and 1041.688 Å. To set limits on the flux of C II* and O VI, we include the airglow lines in our model spectrum, but limit their fluxes to that observed in the O I $\lambda 1027.43$ line, which is generally much brighter than either of the two longer-wavelength features. The resulting limits are higher than those for the nearby Ly β and O VI $\lambda 1031.93$ lines. Fortunately, all of the Virgo data were obtained during orbital night, when the O I line flux is minimal.

Finally, we set upper limits on the FUV continuum emission from each cluster of galaxies. We consider only the region between 1060 and 1070 Å, which is free of airglow features and for which the LiF 1A detector has $A_{\text{eff}} > 20 \text{ cm}^2$. For each observation, we determine the mean background-event rate from unilluminated regions of the detector directly above and below the LWRS extraction window. Scaling these rates to the size of the LWRS window, we find that the observed continuum exceeds the detector background by 110 ± 250 and 200 ± 400 photons $\text{cm}^{-2} \text{ s}^{-1} \text{ Å}^{-1} \text{ sr}^{-1}$, respectively, for Coma and Virgo. (We ignore possible structure in the detector background, thought to be present at the 10% level.)

4. DISCUSSION

4.1. The Coma Cluster

From simultaneous fits to *EUVE* Deep Survey (DS) and *ROSAT*PSPC observations of the Coma cluster, Lieu et al. (1996a) derive the temperature and emission integral as a function of radius for a three-component ICM assuming a distance of 139 Mpc and an abundance $Z = 0.21 Z_{\odot}$ (Hughes et al. 1993). They find a temperature of $8.7 \times 10^5 \text{ K}$ and an emission integral of $4.8 \times 10^{65} \text{ cm}^{-3}$ for the coolest component within $3'$ of the cluster center. Combining these parameters with line emissivities estimated with the CHIANTI software package (Dere et al. 1997) using the Feldman et al. (1992) solar abundances scaled to the assumed cluster metallicity, we derive an expected O VI $\lambda 1032$ flux of 3.8×10^{-3} photons $\text{cm}^{-2} \text{ s}^{-1}$. If the O VI emission were evenly distributed within this region (an assumption consistent with both EUV and soft X-ray maps of the cluster; Bonamente 2000; Briel et al. 1992), then its surface brightness would be 1600 photons $\text{cm}^{-2} \text{ s}^{-1} \text{ sr}^{-1}$, slightly less than our $3\text{-}\sigma$ upper limit to the dereddened O VI surface brightness.

The O VI line emissivity depends critically on the gas temperature. From our limit to the O VI flux of Coma, we derive an upper limit to the emission integral as a function of temperature. In Fig. 2, we compare this limit with the best-fit value of the emission integral derived by Lieu et al. (1996a) for the central region ($r < 3'$) of the cluster,

scaled to the area of the LWRS slit. This value of the emission integral, $EI = 4.2 \times 10^{63} \text{ cm}^{-3}$, lies just below the *FUSE* $3\text{-}\sigma$ upper limit. If we instead use a $2\text{-}\sigma$ limit to the O VI flux, we can nominally exclude the warm-gas model of Lieu et al. (1996a). More recent models of the Coma EUV excess do not require a sub- 10^6 K gas. Bonamente (2000) fits the data with a two-component ICM, the cooler of which has a temperature of $2.9 \times 10^6 \text{ K}$. We would not expect significant O VI emission from such a hot gas.

4.2. The Virgo Cluster

Two groups (Lieu et al. 1996b; Bonamente et al. 2001) have modeled the EUV excess in the Virgo cluster with a warm component of the ICM. Both find that its temperature rises with radius, while its emission integral falls. The brightest FUV emission would thus be expected from the cluster center. Unfortunately, the center of the Virgo cluster is occupied by the galaxy M87, and its strong stellar continuum complicates the FUV spectrum of this region (cf., Dixon et al. 1996). We thus consider data taken at larger radii, about $4'.4$ (2242 s) and $6'.0$ (8688 s) from the cluster center. Both Lieu et al. (1996b) and Bonamente et al. (2001) model the warm ICM using a series of concentric annuli. Our inner data point samples the 3–5 arcmin annulus, while our outer point falls in the 5–7 arcmin region. Because 80% of our data comes from the outer annulus, we compare our observations with model predictions for the 5–7 arcmin annulus. We estimate that errors in our derived limits to the emission integral resulting from this simplification are on the order of the uncertainties in the *FUSE* flux calibration.

Our upper limit to the emission integral as a function of temperature is plotted in Fig. 3. Also shown are the best-fit values of the temperature and emission integral of the warm ICM, derived from simultaneous fits to the DS and PSPC data from the 5–7 arcmin annulus of the Virgo cluster by Lieu et al. (1996b) and Bonamente et al. (2001), respectively, scaled to the area of the LWRS slit. The Lieu et al. model parameters are $T = 5.8 \times 10^5 \text{ K}$, $EI = 9.35 \times 10^{61} \text{ cm}^{-3}$, and $Z = 0.454 Z_{\odot}$, values firmly excluded by our limit to the O VI flux. The Bonamente et al. model employs a much warmer gas, with $T = 9.2 \times 10^5 \text{ K}$, $EI = 4.72 \times 10^{61} \text{ cm}^{-3}$, and $Z = 0.5 Z_{\odot}$; these parameters fall just below the *FUSE* $3\text{-}\sigma$ upper limit. If we instead use a $2\text{-}\sigma$ limit to the O VI flux, we can nominally exclude this model as well.

The redshift of M87 ($z = 0.00436$; Smith et al. 2000) is slightly greater than that of the Virgo cluster mean. Near the center of the cluster, the X-ray emission is well centered on M87, and certain asymmetrical features seem correlated with radio emission from the nucleus (Belsole et al. 2001). If, in this region, the cooling flow emits at the redshift M87, the O VI $\lambda 1032$ line would be strongly attenuated by absorption from Galactic C II $\lambda 1036.3$. An upper limit to the emission integral derived from the O VI $\lambda 1038$ line would be approximately twice our quoted value.

5. CONCLUSIONS

We have obtained FUV spectra of two clusters of galaxies with *FUSE*, the *Far Ultraviolet Spectroscopic Explorer*. Neither spectrum shows significant O VI $\lambda\lambda 1032, 1038$ emission at the cluster redshift. Our $2\text{-}\sigma$ upper limits on

the O VI $\lambda 1032$ flux from Coma and Virgo exclude all published warm-gas models of the EUV excess in these clusters and severely constrain the amount of gas at $T \lesssim 8 \times 10^5$ K in either cluster.

We thank R. Shelton and E. Murphy for discussions of *FUSE* data analysis and D. Buote for thoughtful com-

ments on the manuscript. We acknowledge the outstanding efforts of the *FUSE* P.I. team to make this mission successful. This research has made use of NASA's Astrophysics Data System and the NASA/IPAC Extragalactic Database (NED), operated by JPL for NASA. This work is supported by NASA grant NAG 5-5197.

REFERENCES

- Arabadjis, J. S. & Bregman, J. N. 1999, *ApJ*, 514, 607
 Avni, Y. 1976, *ApJ*, 210, 642
 Belsole, E. et al. 2001, *A&A*, 365, L188
 Berghöfer, T. W., Bowyer, S., & Korpela, E. 2000, *ApJ*, 535, 615
 Bonamente, M. 2000, PhD thesis, University of Alabama in Huntsville
 Bonamente, M., Lieu, R., & Mittaz, J. P. D. 2001, *ApJ*, in press ([astro-ph/0011186](#))
 Bowyer, S. & Berghöfer, T. W. 1998, *ApJ*, 506, 502
 Bowyer, S., Berghöfer, T. W., & Korpela, E. J. 1999, *ApJ*, 526, 592
 Bowyer, S., Lieu, R., & Mittaz, J. 1997, in *IAU Symp. 188, The Hot Universe*, ed. K. Koyama, S. Kitamoto, & M. Itoh (Dordrecht: Kluwer), 52
 Briel, U. G., Henry, J. P., & Böhringer, H. 1992, *A&A*, 259, L31
 Cardelli, J. A., Clayton, G. C., & Mathis, J. S. 1989, *ApJ*, 345, 245
 Dere, K. P., Landi, E., Mason, H. E., Monsignori Fossi, B. C., & Young, P. R. 1997, *A&AS*, 125, 149
 Dixon, W. V., Hurwitz, M., & Ferguson, H. C. 1996, *ApJ*, 469, L77
 Dixon, W. V., Sallmen, S., Hurwitz, M., & Lieu, R. 2001, *ApJ*, submitted
 Drake, J. J. 1999, *ApJS*, 122, 269
 Ebeling, H., Edge, A. C., Böhringer, H., Allen, S. W., Crawford, C. S., Fabian, A. C., Voges, W., & Huchra, J. P. 1998, *MNRAS*, 301, 881
 Edgar, R. J. & Chevalier, R. A. 1986, *ApJ*, 310, L27
 Enßlin, T. A., Lieu, R., & Biermann, P. L. 1999, *A&A*, 344, 409
 Fabian, A. C. 1996, *Science*, 271, 1244
 Feldman, U., Mandelbaum, P., Seely, J. F., Doschek, G. A., & Gursky, H. 1992, *ApJS*, 81, 387
 Forman, W. & Jones, C. 1982, *ARA&A*, 20, 547
 Hartigan, P., Raymond, J., & Hartmann, L. 1987, *ApJ*, 316, 323
 Hughes, J. P., Butcher, J. A., Stewart, G. C., & Tanaka, Y. 1993, *ApJ*, 404, 611
 Krick, J., Arabadjis, J. S., & Bregman, J. N. 2000, *BAAS*, 32, 1403
 Kriss, G. A. 1994, in *ASP Conf. Ser. 61, Astronomical Data Analysis Software and Systems III*, ed. D. R. Crabtree, R. J. Hanisch, & J. Barnes (San Francisco: ASP), 437
 Landini, M. & Monsignori Fossi, B. C. 1990, *A&AS*, 82, 229
 Lieu, R., Ip, W.-H., Axford, W. I., & Bonamente, M. 1999, *ApJ*, 510, L25
 Lieu, R., Mittaz, J. P. D., Bowyer, S., Breen, J. O., Lockman, F. J., Murphy, E. M., & Hwang, C.-Y. 1996a, *Science*, 274, 1335
 Lieu, R., Mittaz, J. P. D., Bowyer, S., Lockman, F. J., Hwang, C.-Y., & Schmitt, J. H. M. M. 1996b, *ApJ*, 458, L5
 Mittaz, J. P. D., Lieu, R., & Lockman, F. J. 1998, *ApJ*, 498, L17
 Moos, H. W. et al. 2000, *ApJ*, 538, L1
 Sahnou, D. J. et al. 2000, *ApJ*, 538, L7
 Schlegel, D. J., Finkbeiner, D. P., & Davis, M. 1998, *ApJ*, 500, 525
 Shelton, R. L. et al. 2001, *ApJ*, submitted
 Slavin, J. D., Shull, J. M., & Begelman, M. C. 1993, *ApJ*, 407, 83
 Smith, R. J., Lucey, J. R., Hudson, M. J., Schlegel, D. J., & Davies, R. L. 2000, *MNRAS*, 313, 469
 Struble, M. F. & Rood, H. J. 1999, *ApJS*, 125, 35
 Voit, G. M., Donahue, M., & Slavin, J. D. 1994, *ApJS*, 95, 87

TABLE 1
 $3\text{-}\sigma$ UPPER LIMITS TO FAR-UV EMISSION LINES

Species	Rest Wavelength (\AA)	Coma Limits		Virgo Limits	
		Observed	Dereddened	Observed	Dereddened
S VI	933.38	3200 ^a	3700	4400	7600
C III	977.02	3900	4400	4800	7700
N III	989.80	1600	1800	4700	7400
Ne VI]	999.20	1300	1500	4500	7000
H I (Ly β)	1025.72	1300	1400	2000	3000
O VI	1031.93	1600	1800	1700	2600
C II*	1037.02	1200	1300	2400	3600
O VI	1037.62	1500	1700	2100	3200
Ne V]	1146.1	2200	2400	2900	4000

^aTo minimize contamination of the SiC 2A channel by solar emission, this upper limit is derived only from Coma data taken during orbital night. (All of the Virgo data were taken during orbital night.)

Note. — Units are photons $\text{cm}^{-2} \text{s}^{-1} \text{sr}^{-1}$. Upper limits are derived assuming an intrinsic line width of 40 km s^{-1} (FWHM) at the cluster redshift. Dereddened limits assume a CCM extinction curve with $E(B-V) = 0.008$ for Coma and 0.030 for Virgo and $R_V = 3.1$.

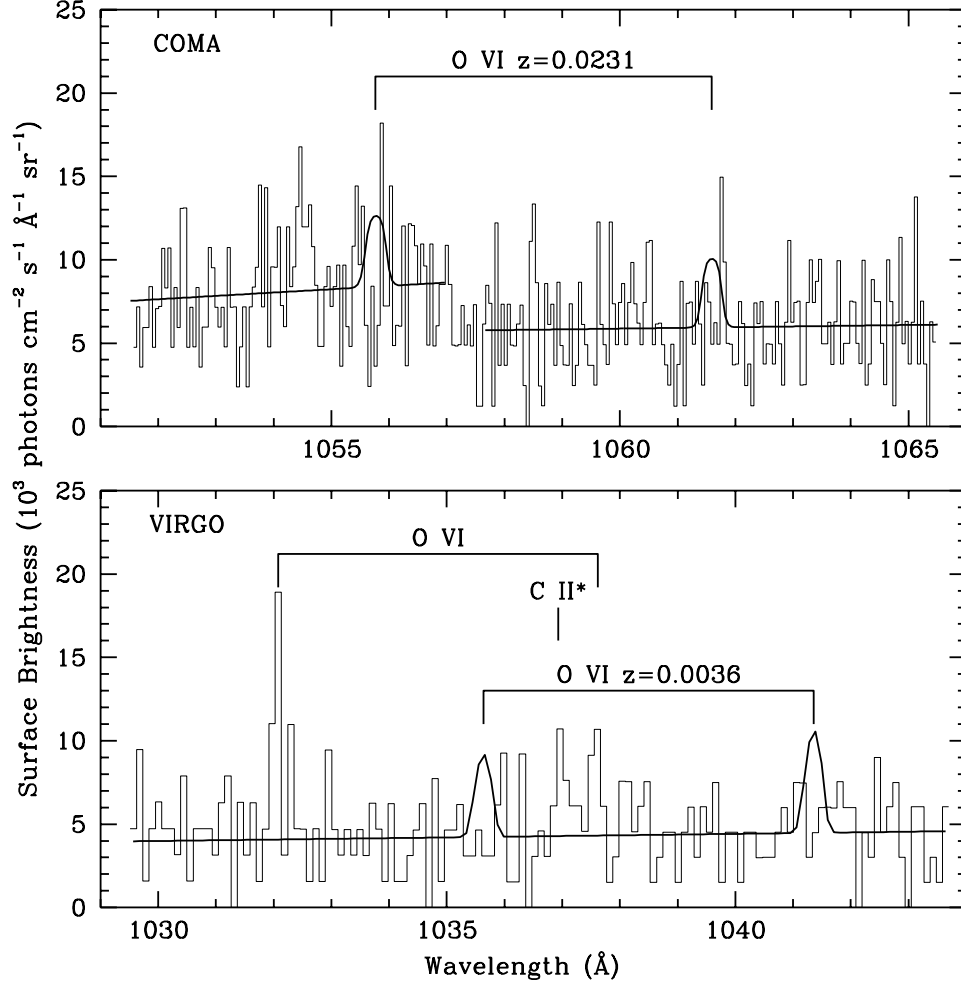


FIG. 1.— *FUSE* spectra of the Coma (top) and Virgo (bottom) clusters, showing the LiF 1A spectrum in the region about redshifted O VI $\lambda\lambda 1032, 1038$. The Coma spectrum is binned by 8 detector pixels, the Virgo spectrum by 16. The data are presented as histograms and are overplotted by models including O VI at our $3\text{-}\sigma$ upper limit. The observed continuum level is consistent with the dark-count rate determined from unilluminated regions of the detector (see text). Wavelengths between 1045 and 1058 \AA are contaminated by stray light on the LiF 1A detector segment; the apparent feature at 1054.5 \AA in the Coma spectrum is thought to be an artifact of the stray-light stripe.

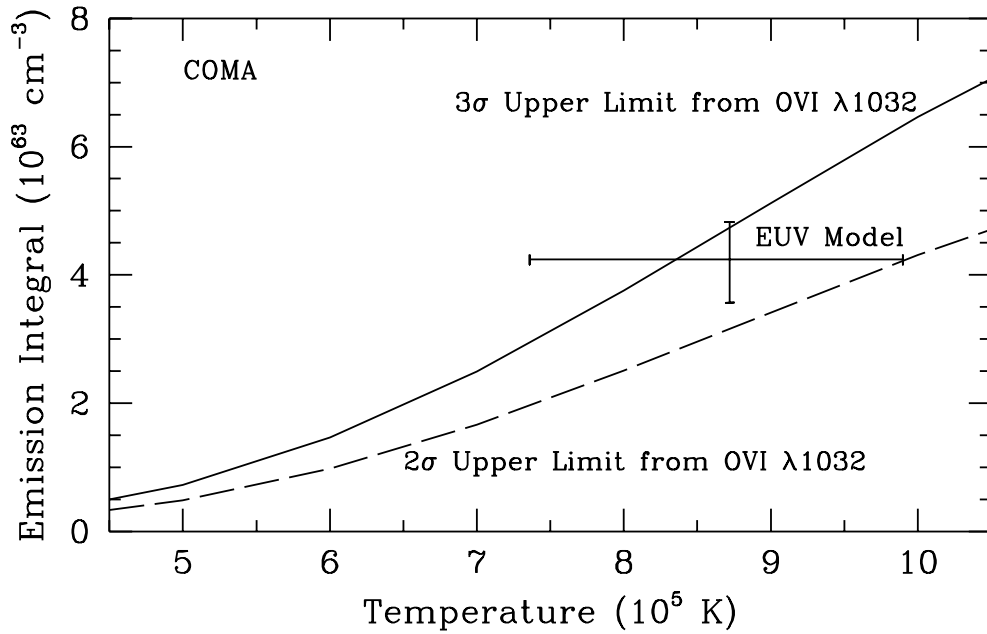


FIG. 2.— Upper limits to the emission integral ($EI \equiv \int n_p n_e dV$) as a function of gas temperature in the Coma cluster. The solid curve is derived from the dereddened 3- σ upper limit to the O VI $\lambda 1032$ surface brightness, assuming the distance (139 Mpc) and abundance ($Z = 0.21 Z_{\odot}$) of Lieu et al. 1996a. The dashed line represents a 2- σ limit to the same feature. The data point indicates the best-fit value of the emission integral and temperature derived for the central region ($r < 3'$) of the cluster by Lieu et al. 1996a, scaled to the area of the *FUSE* LWRS aperture. The *FUSE* data nominally exclude the warm-gas model at the 2-sigma level.

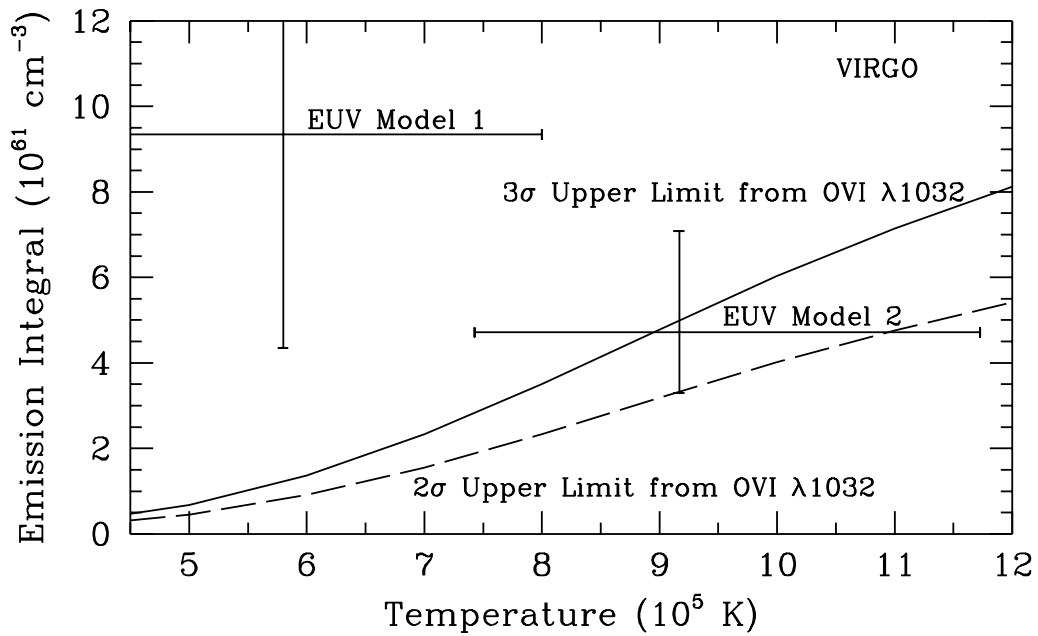


FIG. 3.— Same as Fig. 2, but for Virgo. Our limit to the emission integral assumes the distance (17.2 Mpc) and abundance ($Z = 0.5 Z_{\odot}$) used by Bonamente et al. 2001. The data points indicate the best-fit value of the emission integral and temperature derived for the 5–7 arcmin annulus by Lieu et al. 1996b (EUV Model 1) and Bonamente et al. 2001 (EUV Model 2), scaled to the area of the *FUSE* LWRS aperture and our assumed distance. Model 1 is completely excluded by our limit, while Model 2 is nominally excluded at the 2-sigma level.